Adsorption performance of tartrazine dye from wastewater by raw and modified biomaterial: Equilibrium, isotherms, kinetics and regeneration studies

Adsorption performance of tartrazine dye from wastewater by raw and modified biomaterial: Equilibrium, isotherms, kinetics and regeneration studies

Boutheina Rzig 1, Rouba Kojok 2, Eya Ben Khalifa 1,3,4, Giuliana Magnacca 3,4 , Thouraya Lahssini 2, Bechir Hamrouni 1, Nizar Bellakhal 2

Corresponding author: Eya Ben Khalifa, eya.benkhalifa@unito.it

1 Research Laboratory “Desalination and Water Treatment LR19ES01”, Faculty of Sciences of Tunis, University of Tunis El Manar, 2092 Tunis, Tunisia

2 Ecochimie Laboratory, National Institute of Applied Sciences and Technology (INSAT), University of Carthage, Tunis,Tunisia

3 Department of Chemistry, University of Turin, Via Pietro Giuria 7, 10125 Turin, Italy

4 NIS Interdepartmental Centre, University of Turin, Via Pietro Giuria 7, 10125 Turin, Italy

Abstract

The massive generation of dye waste leads to environmental, social and ecological problems. The use of biomass-derived activated carbon as an adsorbent is a versatile approach that has attracted more attention due to the production of value-added products with lower environmental risk. Application of raw sawdust (SD) and activated sawdust (ASD) for the removal of tartrazine has been investigated. The physicochemical characterization of ASD showed a high surface area, a heterogenous surface with a clear porous structure, and enough functional groups. The effects of various parameters on the removal of the dye were studied. The highest removal percentages were found to be 47.88% for SD and 99.52% for ASD at optimized conditions of pH of 2, temperature of 25 °C, contact time of 60 min, SD mass of 1 g, ASD mass of 0.05 g and 20 mg/L of tartrazine. Langmuir saturation adsorption capacities were equal to 0.8 mg/g for SD and 127 mg/g for ASD at 25 °C. Regeneration of both adsorbents using NaCl showed a decrease in the tartrazine removal from 47.88% to 34.12% for SD and from 99.52% to 70.40% for ASD in five recycle runs. Even if SD shows a more limited efficiency in tartrazine removal, it can be used as it is, without any activation step, therefore it can be a convenient alternative to the activated material. In conclusion, SD and ASD are promising, biodegradable, eco-friendly, cost-effective and efficient adsorbents for the removal of tartrazine from wastewater effluents.

Keywords: Activated sawdust · Biosorption · Tartrazine · Isotherm modelling · Kinetic · Reusability

1 Introduction

Water quality is affected by anthropic activities and one of the most dangerous, despite the regulations, is the direct discharge of dyes from industrial sources. In fact, the high production of dyes can reach 700.000 tons per year and half of these are azo dyes [1, 2]. Tartrazine is one of the most widely used dyes in the industrial sector such as in agrofood, cosmetics and medicine. It can cause abnormal growth of aquatic creatures and poor hatching rates. For example, 100 mM exposure to TTZ showed high toxicity to zebrafish embryos [3]. Obviously, azo dyes are still toxic and carcinogenic to marine animals. This dye has proven to cause negative side-effects on human health like thyroid cancer, asthma attacks, migraines, nervousness, hazy vision and eczema [4]. As a result, water contaminated with dyes causes major concern. In recent years, several techniques were developed to remove these contaminants from wastewater, including advanced oxidative degradation [5], electrocoagulation, electro-Fenton [6], membrane filtration, reverse osmosis [7], electrodialysis [8], precipitation [9], ion exchange [10], and adsorption [11]. However, many of these techniques have limitations, such as high operating and maintenance costs, the production of hazardous sludge, and challenging control of the treatment process [12]. Due to its simplicity and high robustness in removing harmful pollutants like dyes, adsorption has become one of the most used processes [13]. In fact, adsorption using low-cost materials has been demonstrated to be more beneficial than other, more expensive treatment options [14]. The most widely used adsorbent is activated carbon, which has a high capacity for adsorbing a variety of dyes [15]. Many researchers have worked on producing cheap natural activated materials from renewable resources, using low cost methods and precursors, and focusing on decontaminating water in an ecologically friendly way [16]. Many researchers [17–22] have used industrial and agricultural wastes as precursors of activated carbon, but forestry and agricultural wastes are also unused resources that are widely available, making them excellent adsorbent materials. The use of wood generates massive amounts of by-products such as sawdust. About 10 million m3 of sawdust and wood chips are generated annually in Finnish sawmills [23]. Nigeria generates about 1.8 million tonnes of sawdust and 5.2 million tonnes of wood waste annually [24]. In Tunisia, *Pinus halepensis* covers about 297.000 ha, representing more than 56% of the total forest area [25]. *Pinus halepensis* wood sawdust is considered an unimportant waste that is usually thrown away, although it may be collected communally for reuse. Sawdust is an abundant, affordable and easily accessible lignocellulosic material. Many functional groups, including carboxyl and hydroxyl groups, are present in sawdust [26], therefore they are considered ideal precursors for the

synthesis of adsorbing materials. Different studies investigated the use of raw or modified sawdust for the removal of the eriochrome black T dye [27], methylene blue dye [28], crystal violet dye [29]. Helen O. et al. [30] explored the removal of tartrazine and sunset yellow anionic dyes onto activated carbon derived from *cassava sievate* biomass from wastewater. Maximum dye uptake of 20.83 and 0.091 mg/g was recorded for tartrazine and sunset yellow dyes, respectively at pH (1.0–2.0), temperature (30–40 °C), adsorbent mass (0.1 g), and a contact period of 90 min. An extensive literature search revealed that there is currently no research on the use of raw and activated sawdust derived from *Pinus halepensis* wood for the adsorption of tartrazine dye as well as the comparison of their adsorption capacities. In this investigation, the preparation of raw sawdust (SD) and activated sawdust (ASD) for the removal of tartrazine from agro-food wastewater is reported. The produced biosorbents were characterized by scanning electron microscopy (SEM), Fourier transform infrared (FTIR) spectroscopy, gas-volumetric adsorption of nitrogen at 77 K for surface area and porosity determination and thermogravimetric analysis (TGA). In addition, Boehm titration and pH zero charge methods were applied. The effect of adsorption parameters such as pH, contact time, agitation speed, adsorbent mass, initial concentration of dye (tartrazine) and temperature were studied. The adsorption isotherms, kinetics and their changes at different temperatures and different concentrations, respectively, were discussed. The adsorption mechanisms of tartrazine were discussed using the various characterizations of the sorbents. This paper also focuses on the recovery of tartrazine following the adsorption process, which is essential for the long-term use of SD and ASD in the treatment of wastewater.

2 Experimental

2.1 Reagents

The anionic dye tartrazine ((trisodium (4E)-5-oxo-1-(4-sulfonatophenyl)-4-[(4-sulfonatophenyl)hydrazono]-3-pyrazolecarboxylate), commonly known as the additive E102, has a molecular weight of 534.4 g/mol, a molecular formula of C16H9N4Na3O9S2 and was purchased from Sigma Aldrich. Figure 1 displays its chemical structure. Phosphoric acid (85%), sulfuric acid (98%) and hydrochloric acid (37%) were purchased from Acros. Sodium hydroxide and sodium chloride were supplied by Shamlab. All the solutions were prepared with distilled water.

2.2 Preparation of the raw and activated sawdust

Sawdust from *Pinus halepensis* wood (SD) was collected from carpentry located in Ain Draham, Tunisia. It was firstly washed several times with distilled water to remove the surface adhering particles and dried overnight at 80 °C. Then, the completely dried

material was crushed and sieved to obtain a particle size smaller than 200 μ m. The powdered sawdust was chemically activated with concentrated phosphoric acid with an impregnation ratio between the activating agent and the dried sawdust of 1:4 (w/w). The mixture was shaken for one hour at 60 $^{\circ}$ C. The impregnated sample was dried at 105 $^{\circ}$ C and then calcined in a muffle furnace (Protherm furnaces, PLF 110, Ankara, Turkey) at 400 $^{\circ}$ C for one hour with a heating rate of 10 $^{\circ}$ C/min. Similar steps for activation were adopted by Eletta et al. [31]. After cooling, the sample was first washed with hydrochloric acid (0.1 mol/L) for 2 h in order to remove possible residues of calcination and then with distilled water until reaching a neutral pH. This protocol, previously used by S. Hazourli [32], has permitted the cleaning of the micropores of an activated carbon prepared from date stones. The washed sample was dried in the oven overnight at 105 $^{\circ}$ C, placed in an airtight glass bottle and named ASD. Proprieties of the raw sawdust and the activated sawdust were listed in Table 1. Tests of moisture (measured after keeping the sample at 110 $^{\circ}$ C for three hours), ash (after treatment at 900 $^{\circ}$ C for three hours), and volatiles (after treatment at 900 $^{\circ}$ C for seven minutes) were performed [33]. The fixed carbon is given by the remaining portion.

2.3 Physicochemical characterization

The surface morphology of the samples before and after activation was examined using a FEI Quanta 200 scanning electron microscope (Hillsboro, Oregon, United States). FTIR spectra were recorded in the range of 650 - 4000 cm−1, using a Perkin Elmer instrument ≪ Spectrum 100≫ (USA), in attenuated total reflectance (ATR) mode. Thermogravimetric analysis (TGA) was performed on a TA SDT Q600 instrument (USA) with a ramp rate of 10 $^{\circ}$ C/min from 30 to 900 $^{\circ}$ C under nitrogen gas flow of 100 mL/min. The BET specific surface area and pore volume were evaluated using the nitrogen gas-volumetric adsorption measurement at 77 K recorded with an ASAP 2020 Micrometrics instrument, USA (samples before the analyses were outgassed overnight at 30 $^{\circ}$ C for SD and at 250 $^{\circ}$ C for ASD in order to remove the adsorbed atmospheric gases from surface and pores). The pH of zero charge (pHpzc) was also determined by mixing 0.1 g of adsorbent with 5 mL of KNO3 in different flasks and adjusting the pH in the range from 2–10 with HCl or NaOH (0.1 and 1 mol/L). The mixtures were maintained under stirring time of 24 h [34]. The final pH values were recorded using Metrohm pH. The pHpzc was obtained from the intersection of the curve initial pH versus final pH with the bisector.

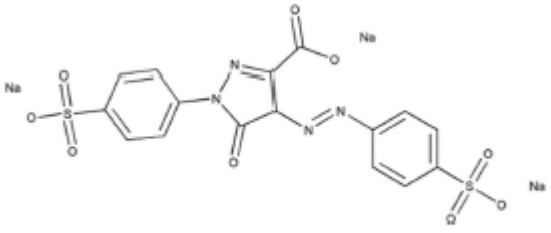

Fig. 1 Chemical structure of tartrazine dye molecule

Table 1 Proximate analysis of SD and ASD

Samples	Moisture (%)	Ash (%)	Volatile matter (%)	Fixed carbon (%)
SD	8 0.69	1.32	82.09	16.59
ASD	10.9	2.52	20.72	76.76

The Boehm titrations were used to evaluate the basic and acidic surface functional groups of SD and ASD [35]. This method is based on the titration of oxygenated functional groups with three different bases, namely sodium carbonate (Na2CO3), sodium bicarbonate (NaHCO3) and sodium hydroxide (NaOH). It allows for the determination of the kinds and quantities of surface functionalities among carboxylic, phenolic, and lactonic surface groups. Briefly, 0.5 g of SD and ASD was placed in different conical flasks. After adding 50 mL of 0.1 mol/L solution of NaOH, NaHCO3 and Na2CO3 (for determination of acidic groups) or 0.1 mol/L HCl (for the determination of basic groups), the mixtures were shaken for 48 h at room temperature. The basic functions were then titrated with HCl (0.1 mol/L) and the acidic groups with NaOH (0.1 mol/L). All experiments were repeated twice. The Thermo Nicolet Flash EA 1112 elemental analyzer, Cambridge, United Kingdom (UK), was used to measure the amounts of C, H, N and S. The oxygen content was determined by difference.

2.4 Dye adsorption experiments

The removal efficiencies of SD and ASD towards tartrazine were investigated by batch adsorption experiments. Tartrazine stock solution (1 g/L) was prepared with distilled water, dilution was applied every day to prepare various solutions. The pH of the solution was adjusted as needed with HCl or NaOH solutions (0.1 and 1 mol/L). Batch adsorption experiments were conducted by placing 50 mL of dye solution in 250 mL of Erlenmeyer conical flasks at required pH value for evaluating the effects of contact time, agitation speed, adsorbent mass, adsorbate concentration and temperature. The removal percentages of tartrazine by the SD and ASD adsorbents were calculated after adsorption. The tartrazine concentration was determined using a Secomam Uv-Light-1469 spectrophotometer (Ales, France) at a wavelength of 425 nm [36]. The removal percentage and the uptake capacity qe (mg/g) were calculated according to the equations [37]:

$$\text{Removal}(\%) = \frac{C_o - C_e}{C_o} \times 100 \qquad (1)$$

$$q_e = \frac{(C_0 - C_e).V}{w} \qquad (2)$$

where the initial and equilibrium tartrazine concentrations are C0 and Ce (mg/L), respectively, V (L) is the dye solution volume and w (g) is the dry adsorbent amount.

The adsorption studies were performed in triplicates to assess the results' repeatability.

2.5 Regeneration study

The regeneration experiments were carried out in order to evaluate the economic validity of the adsorption process. In this study, 1 g of SD and 0.05 g of ASD were treated with 20 mg/L of tartrazine solution for 1 h at the optimum conditions (pH = 2 and T = 25 ° C). Dye loaded adsorbents were filtered then dried overnight at 80 ° C. To test the reusability and regeneration capability of the material, five cycles of the adsorption process were performed using the same adsorbent. Different solutions of NaCl (0.1 M), NaOH (0.1 M), H2SO4 (0.1 M), H3PO4 (0.1 M), HCl (0.1 M) and distilled water were tested during two cycles of regeneration in order to choose the suitable solvent for tartrazine desorption. For the remaining three cycles, only the solution with the best regeneration capacity was used.

3 Results and discussion

3.1 Characterization of raw and activated material

Thermogravimetric analysis is an essential method for establishing the activation temperature to produce activated material and for studying the thermal behavior of the precursor. Figure 2 shows the thermogravimetric (TG) and derivative thermogravimetric (DTG) analyses of sawdust. The first weight loss observed below 200 ° C corresponds to the release of water vapor due to the sample's drying. The second decomposition step in the temperature range of 200 to 350 ° C could be attributed to the hemicellulose. The third stage was mainly attributed to the degradation of cellulose. Compared to hemicellulose, cellulose degrades at a higher temperature range (about 325 to 400 ° C) [38]. The two peaks of hemicellulose and cellulose in the curve (shown in Fig. 2) are not significantly differentiated. The decomposition of hemicellulose is often observed as a more or less pronounced "shoulder" and can also be attributed to the partial decomposition of cellulose and lignin [39]. Finally, the fourth stage of decomposition is attributed to the slow degradation of lignin. Lignin degradation generally occurs over a wide temperature range from 180 to 900 ° C [40]. During the activation process, hemicelluloses and cellulose, volatile substances, oil, gases and activated biomass are produced. After 400 ° C, the weight loss is negligible; therefore, the calcination temperature to prepare the activated sawdust was fixed at 400 ° C. Martin-Lara et al. [40] found similar results in their study, including a weight loss in the first stage due to water evaporation and losses in the following stages due to the decomposition of hemicellulose, cellulose and lignin. The pHpzc is used to better understand the electrostatic interactions during the adsorption process of tartrazine dye.

As shown in Fig. 3, the pH of zero charge of SD and ASD is 4.34 and 2.38, respectively. Therefore, both adsorbents have an acidic nature. The chemical composition of raw and activated sawdust is summarized in Table 2. According to Boehm's titration, the total quantity of acid functions is greater than that of the basic functions for both adsorbents. This confirms the acidic character of the SD and the ASD. This conclusion is consistent with the pHpzc found previously. For SD, the carboxylic functions represent 14%, the lactones 52.50% and the phenolic functions 33.31%. However, the carboxylic functions represent 32%, the lactones 29.33% and the phenolic functions 38.67% of the ASD. It is also clear that after activation of the biomass sample, there was an increase in the amount of carboxylic, lactonic and phenolic groups. This indicated that H3PO4 affected the acid functions in the activation process and the oxidizing atmosphere during the pyrolysis could enhance their amount. Ozcimen and Ersoy-Mericboyu observed similar results for activated carbons prepared from hazelnut shell and apricot stone waste [41]. According to the elemental analysis, the carbon content increased after activation. The carbon content improved from 46.16% to 56.59% while, the hydrogen, nitrogen and oxygen to 41.25, respectively. This is due to the fact that the calcination process causes a release of volatile compounds, such as water and small hydrocarbons [42, 43]. This is also confirmed by the low values of O/C and H/C ratios for the ASD.

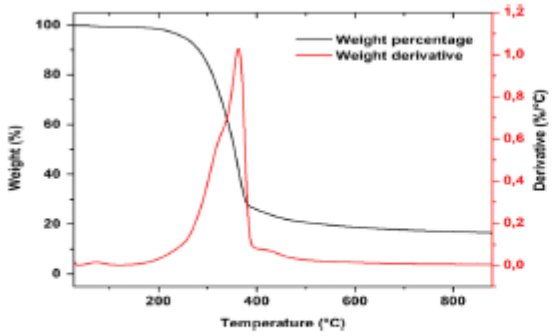

Fig. 2 TG and DTG plots of sawdust (SD)

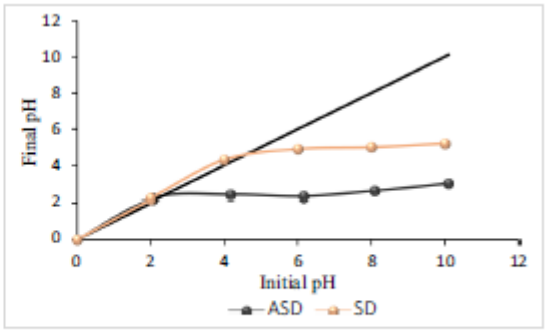

Fig. 3 pH of zero charge of SD and ASD

Table 2 Chemical proprieties of the raw and the activated sawdust

Chemical proprieties	SD	ASD
Boehm titration		
Total of acid functions (mmol/g)	3.52	7.50
Carboxylic (mmol/g)	0.50	2.40
Lactones (mmol/g)	1.85	2.20
Phenol (mmol/g)	1.17	2.90
Total of basic functions (mmol/g)	1.00	1.50
Elemental analysis		
Carbon (%)	46.16 ± 10.39	56.59 ± 0.12
Hydrogen (%)	5.46 ± 0.84	2.08 ± 0.26
Oxygen (%)	48.19 ± 11.22	41.25 ± 0.38
Nitrogen (%)	0.19 ± 0.05	0.07 ± 0.06
Sulfur (%)	0.00 ± 0.00	0.01 ± 0.01
Molar H/C	0.11	0.04
Molar O/C	1.04	0.73

Figure 4 shows the FTIR spectra of tartrazine, SD and ASD before and after adsorption of tartrazine. The large band between 3100 and 3400 cm−1 appearing in the raw material is assigned to OH stretching of carboxyl, phenol and alcohol vibration related to lignin, cellulose, and hemicellulose present in wood products or adsorbed water [44, 45]. The band around 2900 cm−1 is related to symmetric and asymmetric stretching of aliphatic C-H, characteristic of lignocellulosic materials [46]. This peak has disappeared after the activation of the sawdust, indicating the development of aromatics inside the carbon. The appearance of broad band in the ASD spectrum at 1575 cm−1 confirms the presence of C = C aromatic rings [47]. The activated biomass shows an absorption band at 1703 cm−1 due to the C = O groups of the oxidized carbon. In the region between 1100 to 1300 cm−1, a broad peak is observed which could be attributed to C-O stretching of acids, alcohols, ethers, and esters groups. This is in accordance with the results of the Boehm titration and the pH of zero charge, suggesting the increase of acidic groups after activation with phosphoric acid and pyrolysis under an airy atmosphere. Wang et al. [48] explained that the increase in the acidity of carbon upon acid treatment may be attributed to the removal of inorganic compounds leaving sites on the carbon surface that can chemisorb oxygen. Peaks indicated with red arrows in the spectrum of activated sawdust after adsorption could be related to the fingerprint region of the tartrazine spectrum. These peaks are shifted in comparison to the dye spectrum, confirming the involvement of the ASD of carbon functional groups in dye adsorption.

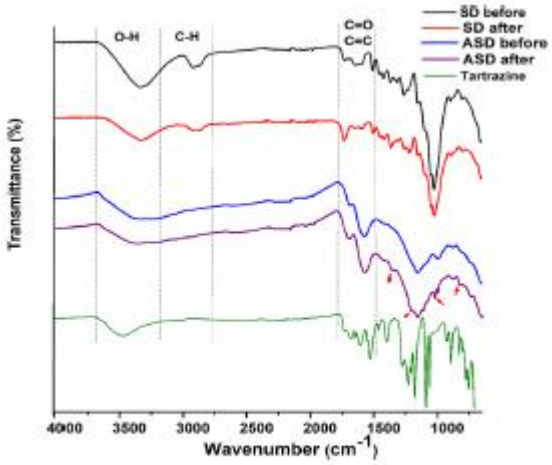

Fig. 4 FTIR spectra of tartrazine, SD before and after adsorption and ASD and after adsorption

The N2 adsorption–desorption isotherms on ASD are presented in Fig. 5. The N2 uptake increased sharply in the low relative pressure ratio ($p/p0 \leq 0.1$), confirming the presence of micropores in ASD [49]. A type 4 hysteresis loop is observed from $p/p0 \geq 0.4$, indicating the development of mesopores inside the biochar [49].

The pore size distribution was calculated using the DFT method and the results are listed in Table 3. The obtained results indicate the development of high porosity in the material with a total pore volume of 0.661 cm3/g, which could be explained by the role of phosphoric acid in the pyrolysis process. M. Lewoyehu [50] demonstrated that H3PO4 has two roles during the activation of the biochars: promotes the dehydration, hydrolysis, and condensation reactions and acts as template by occupying a volume in the interior of the activated precursor. The BET surface area of ASD was 931 m2/g, confirming the effectiveness of acid chemical activation in the development of highly porous materials without the use of high heating during carbonization [50]. Similar results were obtained by Jawad et al. [51] during their work on the synthesis of biochar from phosphoric acid modified coconut leaves for methylene blue (SBET = 941 m2/g).

Scanning electron microscopy analysis has been a primary tool for analyzing the surface morphology and fundamental physical properties of the adsorbent. SEM images of SD and ASD are shown in Fig. 6. Generally, hardwood material shows the existence of elongated, tight fibers, whereas softwood displays tracheids, which are horizontal tubes, as shown in Fig. 6a for the raw sawdust [52, 53]. It is evident that both adsorbents have a heterogeneous surface. This structure is very compact, especially for ASD. Compared to the surface of the raw sorbent, the ASD has developed a large porosity due to the chemical activation with H3PO4 which can lead to the decomposition of labile compounds during the process and the volatilization of organic compounds [54]. This suggests a very high adsorption capacity for this material. In this context, Sieliechi et al. have shown that after activation, the surface of the synthesized material undergoes an important development of the pores [55].

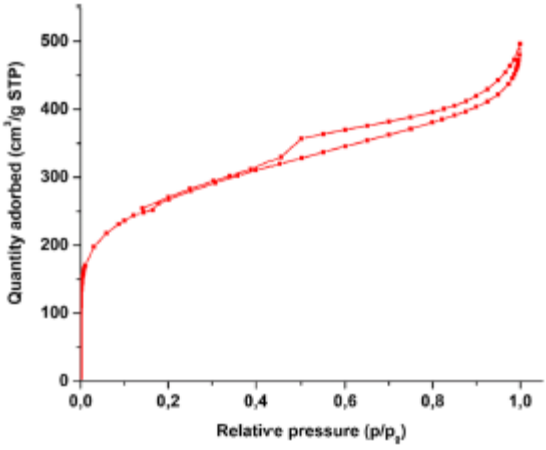

Fig. 5 N_2 adsorption–desorption isotherms at 77 K

Table 3 Textural parameters of the activated sawdust (ASD)

	S_{BET} (m^2/g)	V_{total} (cm^3/g)	V_{meso} (cm^3/g)	V_{micro} (cm^3/g)	Pore diameter (Å)
ASD	931	0.661	0.406	0.255	28.7

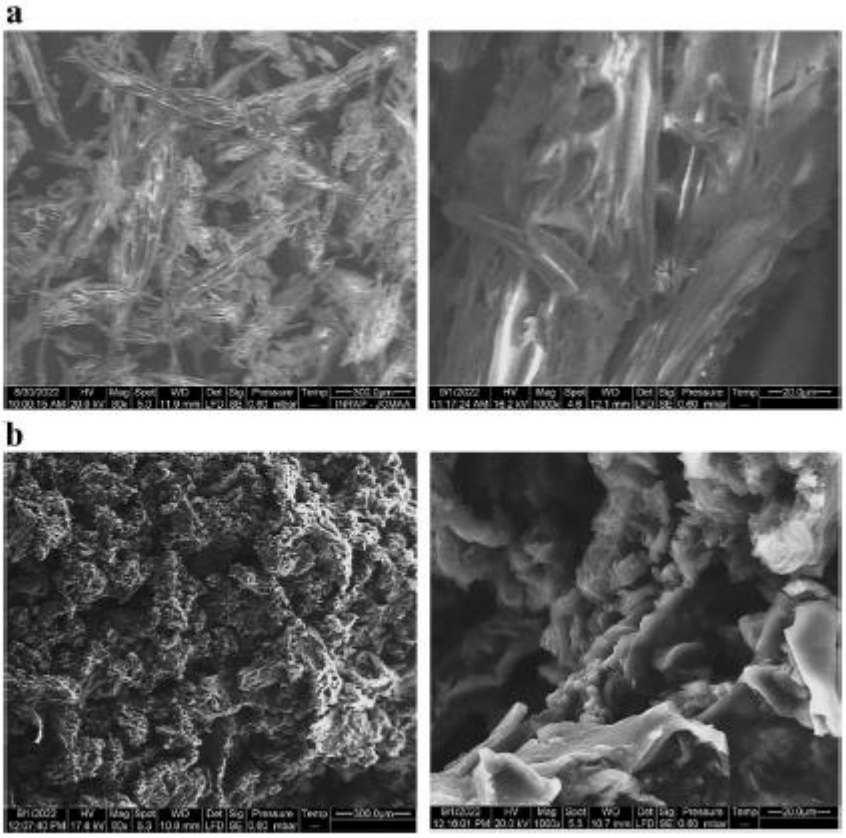

Fig. 6 SEM images **a** Sawdust, **b** Activated sawdust obtained at different magnifications

3.2 Optimization of tartrazine adsorption parameters

The effect of pH, contact time and agitation speed were evaluated considering the amounts of SD and ASD producing comparable responses in term of removal percentage, namely 1 g of SD and 0.01 g of ASD dispersed in 50 mL of agitation speed related to the optimal activity were then applied to evaluate the effect of adsorbent mass and therefore, optimize the amount of materials needed to achieve the best performance in tartrazine removal: those optimized amounts were used in the rest of the study.

3.2.1 Effect of the pH

The pH is a very important factor to take into consideration in adsorption studies as it has an impact on the ionization status of the adsorbent's surface. The determination of the pH of the point zero charge (pHPZC) allows for a better understanding of the ionization of functional groups and their consequent interactions with the adsorbate. Figure 3 shows that it is slightly acidic (4.34) for SD and strongly acidic (2.38) for ASD. The effect of pH on

tartrazine removal was investigated in the pH range from 2 to 10 (in the region where the material's surface changes from positive to negative) using the initial concentration of 20 mg/L as shown in Fig. 7. Given the higher activity shown by ASD materials, all the experiments described below were performed using a lower amount of ASD material with respect to SD material, namely 20 g/L and 0.2 g/L, respectively, supposing, at least in the first approximation, the surface charge at pH = 2 is enough positive to avoid the aggregation of the adsorbing particles (which can affect the adsorbing capacity) in the higher concentration suspensions. The effect of the adsorbent amount will be considered in more details in paragraph 3.2.4. The produced activated sawdust was evidently much more active than SD in the entire range of examined pHs, with the highest adsorption capacity at pH 2.0. Both samples show a sharp decrease of efficiency when raising pH from 2.0 to 7.0. The adsorption capacity completely disappears at pH = 8 for SD and pH = 10 for ASD. This can be explained by the strong electrostatic force of attraction between the negatively charged dye and the positively charged surface of adsorbents at lower pH ranges [56], but also by considering that H+ ions can interact with the negative surface of the adsorbents decreasing the net charge of the surface, avoiding the immediate adsorption of tartrazine molecules at the surface of the adsorbents and allowing an easy diffusion of the molecules into the pores of the materials giving a more efficient adsorption at low pHs [25, 26]. Nevertheless, other less important phenomena, for instance, based on dispersion forces, should be taken into account to explain the removal of the tartrazine, lower but not negligible, at a pH higher than the pHPZC. The trend of the curves reported in Fig. 7 allows some additional considerations. A) The curves run almost in parallel with each other, suggesting that similar phenomena control the removal of tartrazine for the two samples. Actually, similar surface groups are present in the two materials, as indicated by the titration method results, therefore electrostatic attraction and dispersion forces are responsible of the removal of tartrazine in both samples. B) It is not possible to exclude that particle aggregation plays a role when a suspension in high concentration is used, as the removal of tartrazine is much less efficient on SD (in a higher amount in the batch experiment) than on ASD (in a lower amount in the batch experiment), but some additional aspects of the adsorption phenomenon will be considered later on. In any case, given the trend of removal, all the adsorption experiments will be carried out at pH = 2 which represents the optimum value for tartrazine removal.

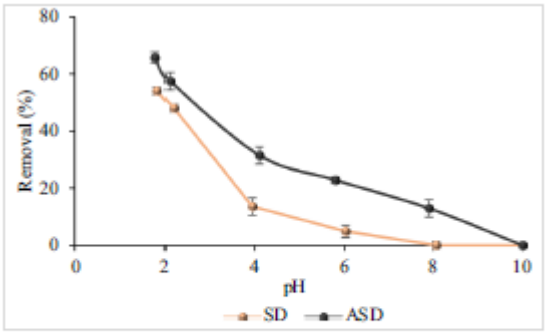

Fig. 7 Effect of pH on tartrazine adsorption for SD and ASD. ([Tartrazine] = 20 mg/L, particle size = 200 µm, T = 25 °C, V = 50 mL, time = 90 min, SD mass = 1 g and ASD mass = 0.01 g)

3.2.2 Effect of contact time

The effect of contact time on the uptake of dyes onto any material is vital in order to detect when equilibrium is attained [57]. The removal of tartrazine by adsorption on SD and ASD was studied as a function of stirring time at 25 ° C and optimal pH. It is clear from Fig. 8 that the removal rate of the dye from solution was first fast and then gradually decreased until equilibrium was reached, after which there was no significant increase in the sorption rate, for both adsorbent. The fast adsorption rate detected at the beginning is attributable to the abundant and vacant surface-active sites on the adsorbent, which get saturated as the time increases [30]. This implies the achievement of adsorption equilibrium, which was reached after 60 min for SD and 50 min for ASD. 60 min was therefore selected for SD and ASD as equilibrium time in the adsorption experiments, as in other similar experiments [58].

3.2.3 Effect of agitation speed

The agitation speed also influences the dye removal from the aqueous solution. Figure 9 shows this effect on the for SD and ASD, mixing speeds of 200 rpm and 400 rpm, respectively, provide the optimum tartrazine adsorption, as a balance between two phenomena: the probability of provoking collisions between the solid and the tartrazine molecules inducing the adsorption phenomenon [59] and the possibility that the collisions are not efficient for the high speed of the particles in the medium. In other words, the adsorbates that were weakly linked to the active site may get detached as the agitation speed increases and rejoin the wastewater mixture [60]. SD and ASD were run at speeds of 200 rpm and 400 rpm, respectively.

3.2.4 Effect of adsorbent mass

Several amounts of SD (ranging between 0.1 and 2 g) and ASD (ranging from 0.01 and 0.1 g) were examined to determine the best amount of adsorbent for tartrazine removal.

The obtained data (Fig. 10) show that the removal percentage of tartrazine is lower for SD than for ASD samples, due to the beneficial impacts that the activation process offers. Moreover, the removal rises gradually with the increase of adsorbent mass, reaching 99.52% for ASD and 47.88% for SD with 0.05 g and 1 g, respectively, as expected considering the increase in adsorbing sites (or surface area) with increasing the mass of the adsorbents [61]. A further increase of the adsorbents' amount does not allow increasing the tartrazine removal, probably, this is caused by the aggregation of material particles limiting the adsorption. Therefore, a mass of 1 g of SD and 0.05 g of ASD were chosen for the following experiments.

3.2.5 Effect of initial dye concentration

The results of the impact of the initial dye concentration on the adsorption process are presented in Fig. 11. The tartrazine removal percentage with SD decreases with the increase in the initial dye concentration, in fact, with high concentrations, the large number of pollutant molecules exceeds the number of available adsorption sites, leading to saturation of the adsorbent [62]. Otherwise, for ASD the concentration of the dye can be increased up to 80 mg/L without any effect on the removal percentage, indicating the presence of many active sites and proving the great capacity of ASD to adsorb pollutant molecules.

3.2.6 Effect of temperature

To conclude the investigation of parameters potentially influencing tartrazine removal, the effect of temperature was investigated, and tartrazine abatement was studied in the temperature range of 10–80 °C. The results are reported in Fig. 12. The temperature has almost no effect on the dye adsorption yield for both adsorbents, apart from carried out at 10 °C, probably because the mobility of the material particles and dye molecules in the suspension is slightly limited, causing a decrease in the number of collisions and consequently a slightly limited adsorption. Given the observed results, the experiments were performed at room temperature, avoiding the consumption of energy necessary for cooling down or heating up the suspensions.

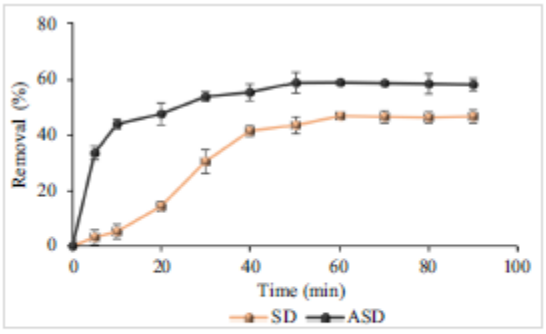

Fig. 8 Effect of time on tartrazine adsorption for SD and ASD. ([Tartrazine]=20 mg/L, pH=2, particle size=200 µm, T=25 °C, V=50 mL, SD mass=1 g and ASD mass=0.01 g)

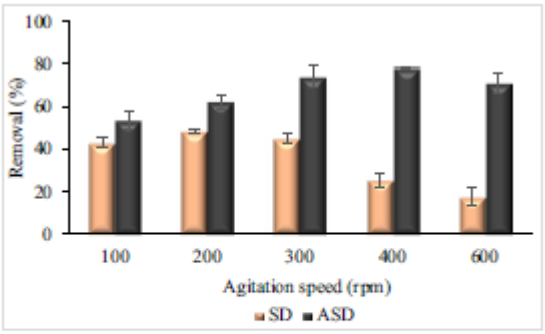

Fig. 9 Effect of agitation speed on tartrazine adsorption for SD and ASD. ([Tartrazine] = 20 mg/L, pH = 2, time = 60 min, particle size = 200 µm, T = 25 °C, V = 50 mL, SD mass = 1 g and ASD mass = 0.01 g)

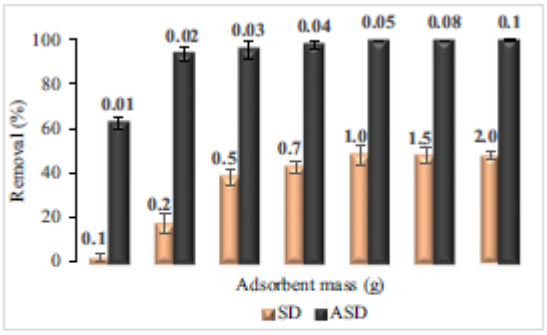

Fig. 10 Effect of adsorbent mass on tartrazine adsorption for SD and ASD. ([Tartrazine] = 20 mg/L, pH = 2, time = 60 min, particle size = 200 µm, T = 25 °C and V = 50 mL.)

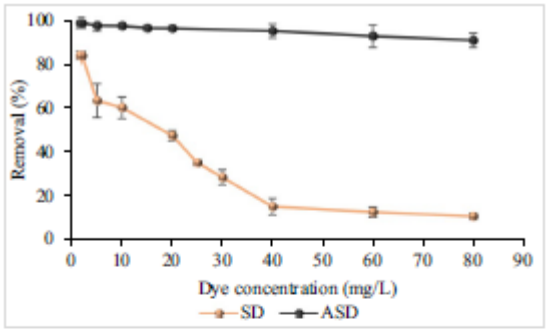

Fig. 11 Effect of initial dye concentration on tartrazine adsorption for SD and ASD. (pH = 2, time = 60 min, particle size = 200 µm, T = 25 °C, V = 50 mL, SD mass = 1 g and ASD mass = 0.05 g)

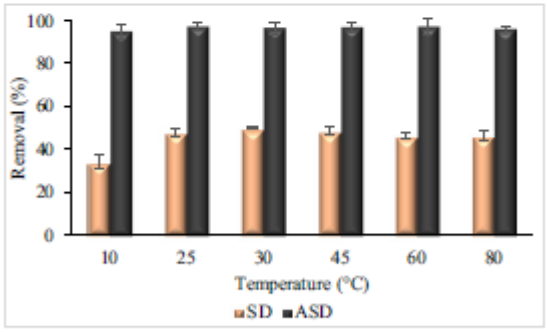

Fig. 12 Effect of temperature on tartrazine adsorption for SD and ASD. ([Tartrazine] = 20 mg/L, pH = 2, time = 60 min, particle size = 200 µm, T = 25 °C, V = 50 mL, SD mass = 1 g and ASD mass = 0.05 g)

3.3 Adsorption kinetics

In order to describe the dye adsorption kinetics on the two adsorbents, the pseudo-first order, pseudo-second order and intra-particular diffusion models were considered to obtain the best fit of our experimental data and therefore to better understand the mechanisms involved in the material-tartrazine interactions. The pseudo-first order model, firstly proposed by Lagergren, is expressed by the nonlinear following equation [63]:

$$q_t = q_e(1 - \exp(-k_1 t)) \quad (3)$$

where qe and qt refer to the adsorption capacity at equilibrium and at time t (mg/g), respectively. k1 (min−1) is the pseudo first order rate constant.

The pseudo-second order model is commonly used for pollutant abatement by adsorption because it allows explaining the kinetics by taking into account the fast and delayed fixation of solutes on the adsorption sites. The nonlinear equation representing this model is the following [64]:

$$q_t = \frac{k_2 q_e^2 t}{1 + k_2 q_e t} \quad (4)$$

where k2 (g/mg min) is the pseudo-second order constant.

The intra-particle diffusion equation is simply presented as follows [65]:

$$q_t = kt^{1/2} + C \quad (5)$$

where Kdif (mg/g min0, 5) is the intraparticle diffusion rate constant and C is the intercept.

The kinetic models' plots are represented in Fig. 13 and the parameters of the different models are listed in Table 4. According to the data shown in Table 4, the pseudosecond order kinetic model has the lowest chi-square χ2 value and the highest R2 correlation coefficient compared to the other models, thus it is the best model to describe the tartrazine adsorption process for both adsorbents. The calculated values qe determined by the pseudo-second order are close to the experimental data (qe,cal = 0.470 mg/g, qe,exp = 0.449 mg/g for SD and qe,cal = 24.000 mg/g, qe,exp = 23.963 mg/g for ASD) and this suggests that the external diffusion or the internal diffusion are the rate-controlling steps in the adsorption process of tartrazine. A similar observation was reported for the adsorption of tartrazine on chitosan/polyaniline system [66].

3.4 Adsorption isotherms

Langmuir, Freundlich, and Dubinin-Astakhov (D-A) adsorption models were used to describe and study the adsorption phenomena of tartrazine on SD and ASD surface at different temperatures.

The most common model for quantifying the amount of adsorbate on an adsorbent as a function of concentration at a given temperature is the Langmuir adsorption model. According to this model, monolayer adsorption of the solute occurs at a fixed number of homogeneously distributed sites on the surface of the adsorbent. The nonlinear equation of the Langmuir isotherm model (Eq. (9)) can be expressed as [67]:

$$q_e = \frac{q_m K_L C_e}{1 + K_L C_e} \qquad (6)$$

where qe is the quantity of tartrazine adsorbed at equilibrium (mg/g), Ce is the equilibrium liquid-phase concentrations of tartrazine dye (mg/L), qm is the maximum monolayer adsorption capacity (mg/g) and KL is the Langmuir isotherm constant (L/mg) that is related to the apparent energy of sorption.

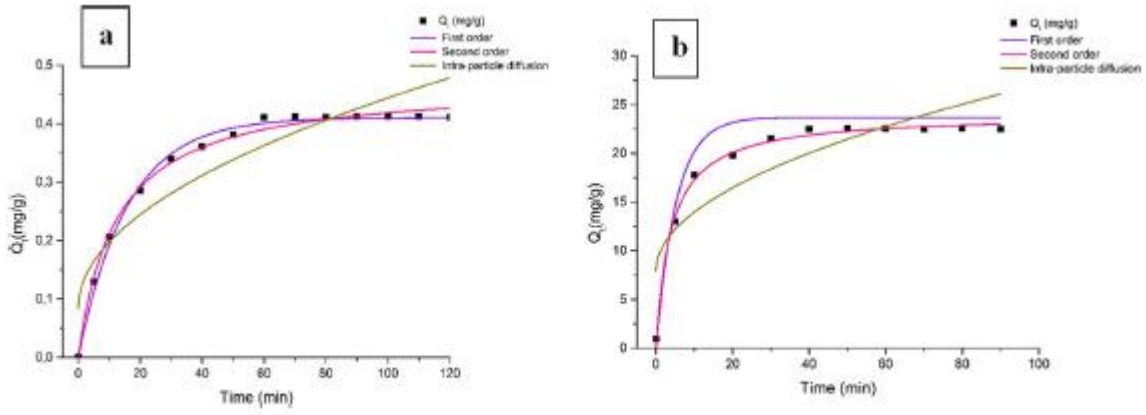

Fig. 13 Adsorption kinetics of tartrazine on **a** SD and **b** ASD

Table 4 Kinetic model parameters for tartrazine adsorption onto SD and ASD. ([Dye] = 20 mg/L, SD mass = 1 g, ASD mass = 0.05 g V = 50 mL and pH = 2 at 25 °C)

Kinetic model	Parameters	Values	
		SD	ASD
Pseudo first order	q_e (mg/g)	0.410	23.696
	k_1 (min^{-1})	0.063	0.190
	R^2	0.994	0.988
	χ^2	0.00	0.57
Pseudo second order	q_e (mg/g)	0.470	24.000
	k_2 (g/mg min)	0.173	0.011
	R^2	0.994	0.994
	χ^2	0.00	0.27
Intra-particle diffusion	k_{dif} (mg/g $min^{0.5}$)	0.036	1.914
	C	0.083	7.918
	R^2	0.855	0.719
	χ^2	0.00	12.51
	$q_{e,exp}$	0.449	23.963

The essential characteristics of the Langmuir isotherm can be expressed by a separation factor (RL), which indicates the nature of the adsorption process and is defined by the following equation [68]:

$$R_L = \frac{1}{1 + K_L C_0} \quad (7)$$

where KL is the Langmuir adsorption constant (L/mg) and Co is the initial concentration of the tartrazine (mg/L). If the RL value falls between 0 and 1, the adsorption is considered favorable, it is unfavorable when this value exceeds 1 and it is irreversible when it is equal to 0 [69].

The Freundlich isotherm is an empirical model based on adsorption on a heterogeneous surface and assumes that the adsorption occurs at sites with different adsorption energies.

The Freundlich model takes the following nonlinear form [70]:

$$q_e = K_F C_e^{\frac{1}{n_F}} \quad (8)$$

where KF (mg/g) and nF represent the adsorption capacity and intensity of the Freundlich model, respectively.

The Dubinin-Astakhov (D-A) model is characterized by the following equation [35]:

$$q_e = q_{DA} \exp\left[-\left(\frac{\varepsilon}{\sqrt{2E}}\right)\right]^{nDA} \text{ with } \varepsilon = RT\,Ln\left(1 + \frac{1}{Ce}\right) \quad (9)$$

Where qe is the quantity of dye adsorbed at equilibrium (mg/g), qDA is the maximum adsorption capacity (mg/g), E is the D-A energy of adsorption (J/mol), nDA is the heterogeneity factor, and ε is the Polanyi potential. R is the gas constant (8.314 J/mol K), T is the temperature in K, and Ce is the adsorbate equilibrium concentration (mg/L).

Figure 14 shows the adsorption isotherms of tartrazine at 25, 35 and 45 $^{\circ}$ C on SD and ASD. Table 5 reports the corresponding coefficients and constants determined for each model.

As suggested by the data reported in Table 5, Langmuir model has the highest correlation coefficient R2 values and the lowest chi-square $\chi 2$ values at all the considered temperatures, therefore, Langmuir is the most appropriate model to describe the adsorption phenomenon of tartrazine on the two adsorbents used. This suggests that the adsorption of tartrazine can occur through the formation of a monolayer of adsorbed molecules on the active sites of the materials [71]. The values of the separation factor (RL) are between 0 and 1 (Table 5), suggesting favorable tartrazine adsorption onto both

adsorbents. Other interesting information can be gathered by applying the other models to the adsorption values. For instance, the values of 1/nF shown in Table 5 are smaller than 1, indicating favorable adsorption of the dye under the studied conditions [72]. The values of the adsorption energy E determined by the D-A model are lower than 8 kJ/mol, indicating a physisorption process [73].

The maximum adsorption capacities according to the Langmuir model are 0.848 and 127.742 mg/g for SD and ASD, respectively, at room temperature. These results are compared with those of other potential biosorbents derived from various ligno-cellulosic biomasses (raw and activated materials) described in the literature (Table 6). According to a literature review, the results of Table 6 demonstrate that commercially produced artificial adsorbents and activated carbon derived from biomass are very efficient in tartrazine removal. It is also clear that the activated sawdust (ASD) studied in this work has a very good affinity towards tartrazine compared to other activated carbons reported in the Table 4. Thus, the abundant and sustained availability of SD biomass along with its desirable tartrazine biosorption characteristics guarantees a promising and reliable technique for the treatment of tartrazine dye from aqueous streams.

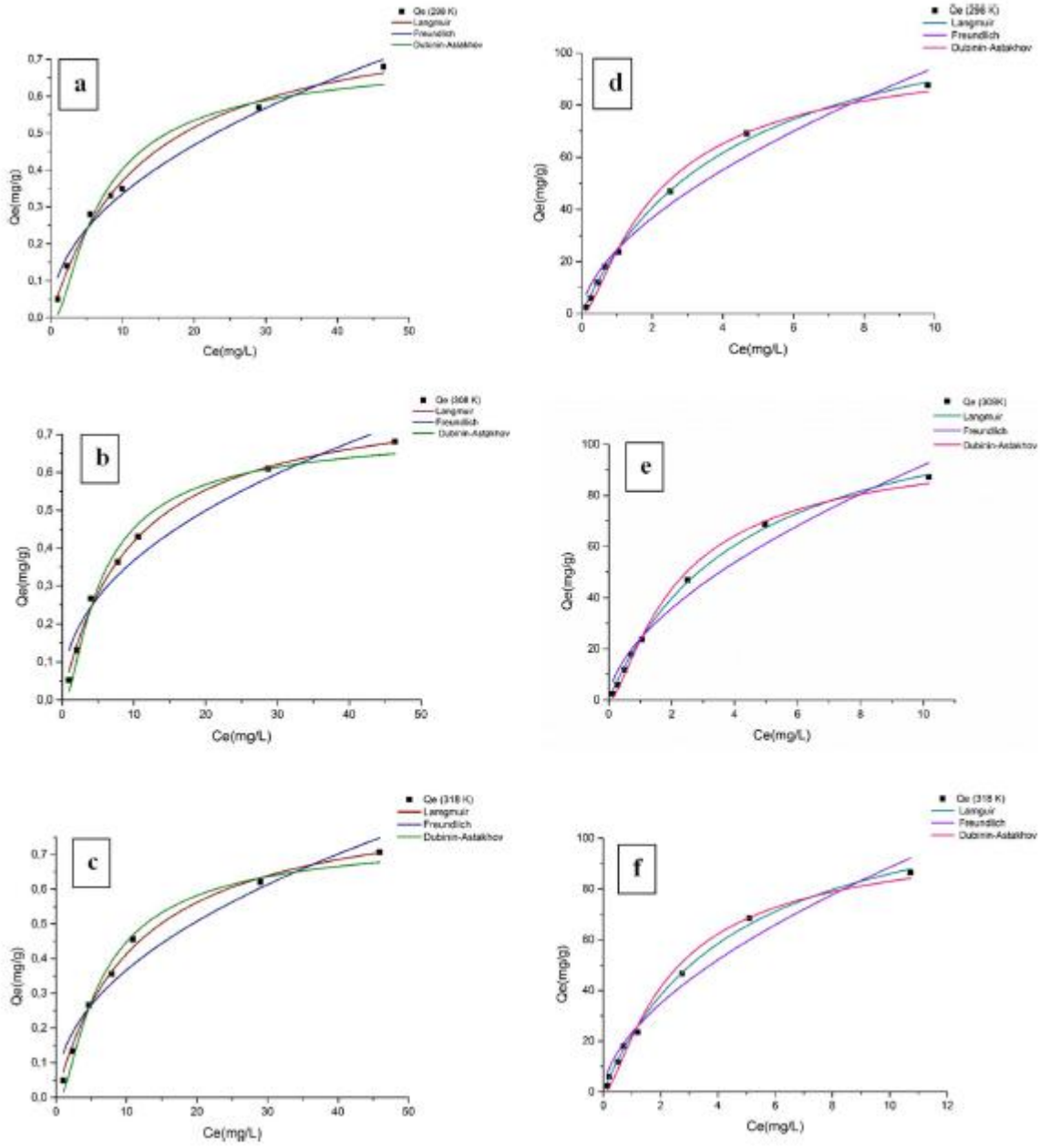

Fig. 14 Adsorption isotherms of tartrazine on SD and ASD, respectively at **a, d** 298 K; **b, e** 308 K and **c, f** 318 K

Table 5 Isotherm model parameters for the adsorption of tartrazine onto SD and ASD. (SD mass = 1 g, ASD mass = 0.05 g V = 50 mL, pH = 2 and contact time = 1 h at 25, 35 and 45 °C)

Model	Parameters	SD			ASD		
		25 °C	35 °C	45 °C	25 °C	35 °C	45 °C
Langmuir	K_L (L/mg)	0.078	0.103	0.089	0.233	0.231	0.218
	q_m (mg/g)	0.848	0.821	0.877	127.742	125.825	125.400
	R^2	0.992	0.995	0.994	0.998	0.998	0.997
	χ^2	3.84	0.00	0.00	2.31	1.64	3.13
	R_L	[0.865-0.1338]	[0.829–0.108]	[0.849–0.123]	[0.682–0.051]	[0.684–0.051]	[0.696–0.054]
Freundlich	K_F (L/mg)	0.111	0.132	0.125	24.439	23.858	23.315
	n_F	2.087	2.258	2.144	1.703	1.709	1.726
	R^2	0.975	0.941	0.942	0.967	0.967	0.967
	χ^2	0.00	0.00	0.00	32.83	32.39	31.28
D-A	q_{DA} (mg/g)	0.719	0.720	0.764	104.786	103.644	102.904
	n_{DA}	2.453	1.945	1.999	2.210	1.458	1.102
	E (kJ/mol)	0.498	0.519	0.444	3.321	2.114	1.833
	R^2	0.938	0.975	0.982	0.989	0.992	0.984
	χ^2	0.00	0.00	0.00	11.07	12.92	15.38

Table 6 Comparative analysis of tartrazine biosorption by various biosorbents

Biosorbent	pH	Dose (g/L)	Temperature (°C)	[Dye] (mg/L)	Capacity (mg/g)	Ref
Sawdust	3	5	35	1	1.4	[49]
Lantana Camara	2	0.2	50	25	90.90	[58]
Pecan nuts shells	-	1	20	0.1	64.2	[71]
Nigerian soil	2	1.25	50	50	83.33	[74]
Commercial activated carbon	5	10	25	200	121.3	[75]
Commercial activated carbon	2	2	23	5	3.32	[76]
Activated carbon derived from cassava sievate	2	0.1	40	150	20.83	[30]
Activated carbon-doped magnetic nanocomposites	2	2	70	10	435.72	[77]
Activated carbon prepared from cola nut shells	2	0.5	25	20	24.57	[78]
Sawdust (SD)	2	20	25	20	0.88	This study
Activated sawdust (ASD)	2	1	25	20	127.82	This study

Table 7 shows a comparison of raw and activated sawdust performance for different dye removals. This comparison proved that sawdust is inexpensive, has good performance and appears to be enough for treating wastewater containing persistent dye contaminants.

Table 7 Comparison of the maximum adsorption capacities of raw and activated sawdust for the removal of different dyes

	Dye	pH	Dose (g/L)	Temperature (°C)	[Dye] (mg/L)	Capacity (mg/g)	Ref
Raw sawdust	Methylene blue	10.5	15	25	300	14.00	[79]
	Syncozol Red	3	1	25	15	21.71	[80]
	Basic Blue 3	4.3	10	25	50	28.69	[81]
	Orange G	2	1	35	2.5	0.24	[82]
	crystal violet	7.5	0.8	55	200	129.77	[83]
	Tartrazine	2	20	25	20	0.88	This study
Activated sawdust	Remazol Brilliant Violet 5R	7	1	30	100	204.08	[84]
	Orange G	2	1	35	2.5	0.40	[82]
	methylene blue	8	5	30	500	47.62	[85]
	Tartrazine	2	1	25	20	127.82	This study

Adsorption process of anionic dyes could be assigned to diverse types of interactions: electrostatic attraction, π - π interaction, hydrogen bonding, Van der Waals force [86]. A possible model of the adsorption mechanism is proposed in Fig. 15, specifying the main interactions occurring between the ASD and tartrazine.

ASD presented a porous structure with a high surface specific area equal to 931 m2/g. Physisorption of tartrazine can be performed through filling the pores developed in the synthesized biochar [87]. Attraction and repulsion interactions that occurred during the adsorption process are presented in the mechanism above. Sulfonate and carboxylic groups present in tartrazine are responsible for its anionic character, which attracts the positively charged surface of ASD at pH less than the pH of zero charge (2,38) [88]. The FTIR analysis revealed that ASD possesses a graphitic structure enriched with electron-donor functional groups like hydroxyl and carbonyl groups. These aromatic cycles can interact with the benzene ring structure of the dye through π - π interaction [89]. Furthermore, the adsorption process can involve the formation of hydrogen bonds between the carbonyl groups of the dye and the functional groups present in activated biochar [90].

3.6 Effect of recycling adsorbents

Five cycles of the adsorption process were performed under optimal adsorption conditions to test the reusability and regeneration competence of the materials. Different solutions, namely NaCl (0.1 M), NaOH (0.1 M), H2SO4 (0.1 M), H3PO4 (0.1 M) and HCl (0.1 M) in distilled water, were tested during two cycles of regeneration in order to choose the suitable solvent for desorption of tartrazine. For the remaining cycles, only the solution with optimal removal was used. Figure 16 shows the results of the regeneration of the two adsorbents compared with the adsorption capacity of the materials before the regeneration.

The results show that NaCl is the best solution for regenerating both adsorbents because it can interact with tartrazine (associating Na + ions to the molecules' negatively charged sulfonate groups, limiting interaction with solids) and adsorbent materials (associating Cl- ions to the adsorbing sites, which are less available to keep adsorbate molecules blocked at the surface) [59, 60]. The regeneration mechanism can be explained by the electrostatic interaction between the negatively charged functional groups (OH^-, COO^-) the Na^+ ions of the dissociated NaCl [91]. The same charges on the adsorbent surface between the two formed a repulsive electrostatic force, reduced the effectiveness of the adsorption process. The dye removal after regeneration decreases from 47.88% to 34.12% for SD and from 99.52% to 70.40% for ASD after the fifth cycle but both are still acceptable. At the end of their lives, both SD and ASD could be burned as fuel.

Fig. 15 Proposed adsorption mechanism of tartrazine on ASD

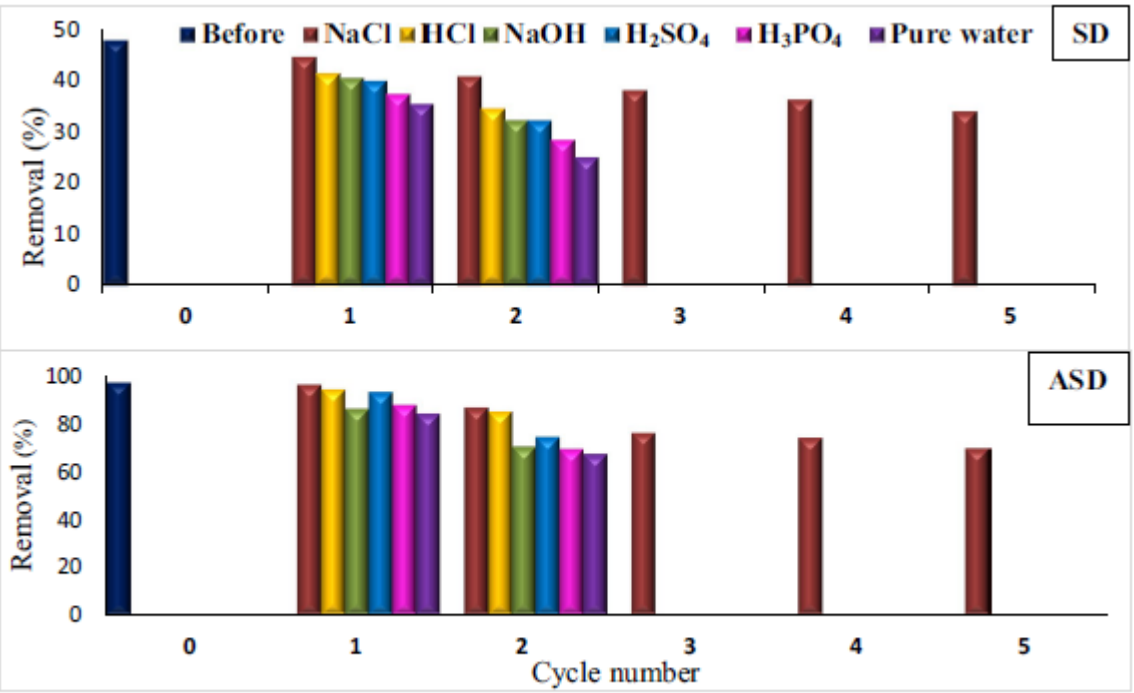

Fig. 16 Regeneration studies of the SD and ASD biosorbents

4 Conclusion

Activated sawdust was prepared from *Pinus halepensis* by chemical activation with H3PO4 followed by calcination in a muffle furnace, characterized and used for the removal of tartrazine dye from aqueous solutions. The activated sawdust showed higher porosity with a higher surface area of 931 m2/g, pore volume and adsorption capacity for tartrazine removal than the raw sawdust. FTIR analysis, Boehm titration and pH of zero charge proved that the prepared carbon is rich in oxygen groups, which enhances its adsorption capacity. The adsorption conditions were optimized in terms of pH, contact time, agitation speed, mass of adsorbent dye initial concentration and temperature. The maximum adsorption was observed at pH 2, and the adsorption attains equilibrium within 60 min. Tartrazine adsorption kinetics followed a pseudo-second order rate model; the Langmuir model well fits the experimental data of both adsorbents, indicating tartrazine sorption in a monolayer. The values of the monolayer maximum adsorption capacity qe,max, were found to be higher for ASD (127.742 mg/g) than SD (0.848 mg/g) at room temperature, which was in accordance with the high surface area, high carbon content and total pore volume of the activated sample. Adsorption mechanisms of tartrazine dye could involve mainly: electrostatic interaction, π - π conjugation, pore filling, Van der Waals force and hydrogen bonding force. Sodium chloride solution at a concentration of 0.1 mol/L was found to be the best solution for regenerating the material's surface and recycling adsorbed tartrazine. SD and ASD can be reused for five dye adsorption runs with a limited lack of the adsorbing capacity. Therefore, these materials are potential options to replace conventional

adsorbents in the water treatment industry. Hence, ASD can be used as a promising adsorbent in this industry. Nevertheless, the application of activated carbon derived from sawdust is still limited and requires increased attention to its properties and processes. Adsorbents with excellent adsorption efficiency and reusability in the removal of dyes from wastewater treatment will be successfully commercialized for the large-scale removal of emerging pollutants from water for the benefit of society.

Funding The authors are thankful to The National Institute of Applied Sciences and Technology (INSAT), University of Carthage 1054, TUNISIA for allowing the research work to be conducted, Department of Chemistry and NIS Interdepartmental Centre, University of Turin for providing necessary instruments for the characterization of the materials.

References

1. Villabona-Ortiz A, Figueroa-Lopez KJ, Ortega-Toro R (2022) Kinetics and Adsorption Equilibrium in the Removal of Azo-Anionic Dyes by Modified Cellulose. Sustainability 14:3640. https:// doi. org/ 10. 3390/ su140 63640

2. de Mattos NR, de Oliveira CR, Camargo LGB et al (2019) Azodye adsorption on anthracite: A view of thermodynamics, kinetics and cosmotropic effects. Sep Purif Technol 209:806–814. https://doi. org/ 10. 1016/j. seppur. 2018. 09. 027

3. Jiang L-L, Li K, Yan D-L et al (2020) Toxicity Assessment of 4 Azo Dyes in Zebrafish Embryos. Int J Toxicol 39:115–123. https://doi. org/ 10. 1177/ 10915 81819 898396

4. Kamal AA, Fawzia SE-S (2018) Toxicological and safety assessment of tartrazine as a synthetic food additive on health biomarkers: A review. Afr J Biotechnol 17:139–149. https:// doi. org/ 10.5897/ AJB20 17. 16300

5. Ben Hafaiedh N, Fourcade F, Bellakhal N, Amrane A (2020) Iron oxide nanoparticles as heterogeneous electro-Fenton catalysts for the removal of AR18 azo dye. Environ Technol 41:2146–2153. https:// doi. org/ 10. 1080/ 09593 330. 2018. 15572 58

6. Priyadarshini M, Ahmad A, Das S, Ghangrekar MM (2022) Application of innovative electrochemical and microbial electrochemical technologies for the efficacious removal of emerging contaminants from wastewater: A review. J Environ Chem Eng 10:108230. https:// doi. org/ 10. 1016/j. jece. 2022. 108230

7. Nain A, Sangili A, Hu S-R et al (2022) Recent progress in nanomaterial-functionalized membranes for removal of pollutants. iScience 25:104616. https:// doi. org/ 10. 1016/j. isci. 2022. 104616

8. Dung NT, Duong LT, Hoa NT et al (2022) A comprehensive study on the heterogeneous electro-Fenton degradation of tartrazine in water using CoFe2O4/carbon felt cathode. Chemosphere 287:132141. https:// doi. org/ 10. 1016/j. chemo sphere. 2021. 132141

9. Bagtash M, Zolgharnein J (2022) Carbon-Magnetic Layered Double Hydroxide as a New Nanosorbent for Efficient Removal of Tartrazine and Indigo Carmine Dyes from Water Solutions; Multivariate Optimization and Adsorption Characterization. J Water Chem Technol 44:259–268. https:// doi. org/ 10. 3103/ S1063 455X2 20400 4X

10. Wu Y, Abdulkreem AL-Huqail A, Farhan ZA et al (2022) Enhanced artificial intelligence for electrochemical sensors in monitoring and removing of azo dyes and food colorant substances. Food Chem Toxicol 113398. https:// doi. org/ 10. 1016/j.fct. 2022. 113398

11. Elgarahy A, Al-wakeel K, Mohammad S, Shoubaky G (2021) A critical review of biosorption of dyes, heavy metals and metalloids from wastewater as an efficient and green process. Clean Eng Technol 4:100209. https:// doi. org/ 10. 1016/j. clet. 2021. 100209

12. Ali K, Javaid MU, Ali Z, Zaghum MJ (2021) Biomass-Derived Adsorbents for Dye and Heavy Metal Removal from Wastewater. Adsorpt Sci X0026 Technol 2021:e9357509. https:// doi. org/ 10.1155/ 2021/ 93575 09

13. Elgarahy AM, Elwakeel KZ, Mohammad SH, Elshoubaky GA (2020) Multifunctional eco-friendly sorbent based on marine brown algae and bivalve shells for subsequent uptake of Congo red dye and copper(II) ions. J Environ Chem Eng 8:103915. https://doi. org/ 10. 1016/j. jece. 2020. 103915

14. Atmani F, Kaci MM, Yeddou-Mezenner N et al (2022) Insights into the physicochemical properties of Sugar Scum as a sustainable biosorbent derived from sugar refinery waste for efficient cationic dye removal. Biomass Convers Biorefinery. https:// doi.org/ 10. 1007/ s13399- 022- 02646-3

15. Fakayode OA, Aboagarib EAA, Zhou C, Ma H (2020) Co-pyrolysis of lignocellulosic and macroalgae biomasses for the production of biochar - A review. Bioresour Technol 297:122408. https:// doi.org/ 10. 1016/j. biort ech. 2019. 122408

16. Husien S, El-taweel RM, Salim AI et al (2022) Review of activated carbon adsorbent material for textile dyes removal: Preparation, and modelling. Curr Res Green Sustain Chem 5:100325. https:// doi. org/ 10. 1016/j. crgsc. 2022. 100325

17. Bilal M, Ali J, Bibi K et al (2022) Remediation of different dyes from textile effluent using activated carbon synthesized from Buxus Wallichiana. Ind Crops Prod 187:115267

18. El-Bery HM, Saleh M, El-Gendy RA et al (2022) High adsorption capacity of phenol and methylene blue using activated carbon derived from lignocellulosic agriculture wastes. Sci Rep 12:1–17

19. Gohr MS, Abd-Elhamid AI, El-Shanshory AA, Soliman HM (2022) Adsorption of cationic dyes onto chemically modified activated carbon: Kinetics and thermodynamic study. J Mol Liq 346:118227

20. Gupta SA, Vishesh Y, Sarvshrestha N et al (2022) Adsorption isotherm studies of Methylene blue using activated carbon of waste fruit peel as an adsorbent. Mater Today Proc 57:1500–1508

21. Khalifa EB, Azaiez S, Magnacca G et al (2022) Synthesis and characterization of promising biochars for hexavalent chromium removal: application of response surface methodology approach. Int J Environ Sci Technol. https:// doi. org/ 10. 1007/s13762- 022-04270-0

22. Sultana M, Rownok MH, Sabrin M et al (2022) A review on experimental chemically modified activated carbon to enhance dye and heavy metals adsorption. Clean Eng Technol 6:100382

23. Rusanen A, Lappalainen K, Karkkainen J et al (2019) Selective hemicellulose hydrolysis of Scots pine sawdust. Biomass Convers Biorefinery 9:283–291. https:// doi. org/ 10. 1007/

s13399- 018- 0357-z

24. Udokpoh U, Nnaji C (2023) Reuse of sawdust in developing countries in the light of sustainable development goals. Recent Prog Mater 5:1-33. https:// doi. org/ 10. 21926/ rpm. 23010 06

25. Sghaier T, Youssef A (2012) Croissance et production du pin d’ Alep (Pinus halepensis Mill.) en Tunisie - Growth and production of Aleppo pine (Pinus halepensis Mill.) in Tunisia. Ecol Mediterr 38:39–57

26. Khalid W, Cheng CK, Liu P et al (2022) Fabrication and characterization of a novel Ba2+-loaded sawdust biochar doped with iron oxide for the super-adsorption of SO42− from wastewater. Chemosphere 303:135233. https:// doi. org/ 10. 1016/j. chemo sphere.2022. 135233

27. Akhouairi S, Ouachtak H, Addi AA et al (2019) Natural Sawdust as Adsorbent for the Eriochrome Black T Dye Removal from Aqueous Solution. Water Air Soil Pollut 230:181. https:// doi. org/10. 1007/ s11270- 019- 4234-6

28. Karthik R, Muthezhilan R, Jaffar Hussain A et al (2016) Effective removal of Methylene Blue dye from water using three different low-cost adsorbents. Desalination Water Treat 57:10626–10631. https:// doi. org/ 10. 1080/ 19443 994. 2015. 10395 98

29. Khattri SD, Singh MK (2012) Use of Sagaun sawdust as an adsorbent for the removal of crystal violet dye from simulated wastewater. Environ Prog Sustain Energy 31:435–442. https:// doi. org/10. 1002/ ep. 10567

30. Chukwuemeka-Okorie HO, Ekuma FK, Akpomie KG et al (2021) Adsorption of tartrazine and sunset yellow anionic dyes onto activated carbon derived from cassava sievate biomass. Appl Water Sci 11:27. https:// doi. org/ 10. 1007/ s13201- 021- 01357-w

31. Eletta OAA, Mustapha SI, Ajayi OA, Ahmed AT (2018) Optimization of dye removal from textile wastewater using activated carbon from sawdust. Niger J Technol Dev 15:26. https:// doi. org/10. 4314/ njtd. v15i1.5

32. Hazourli S, Ziati M, Hazourli A (2009) Characterization of activated carbon prepared from lignocellulosic natural residue:-Example of date stones-. Phys Procedia 2:1039–1043. https:// doi. org/10. 1016/j. phpro. 2009. 11. 060

33. Oladimeji TE, Odunoye BO, FrancisB Elehinafe et al (2021) Production of activated carbon from sawdust and its efficiency in the treatment of sewage water. Heliyon 7:e05960. https:// doi. org/ 10.1016/j. heliy on. 2021. e05960

34. Chakraborty R, Asthana A, Singh AK et al (2022) Chicken feathers derived materials for the removal of chromium from aqueous solutions: kinetics, isotherms, thermodynamics and regeneration studies. J Dispers Sci Technol 43:446–460. https:// doi. org/ 10.1080/ 01932 691. 2020. 18427 60

35. Rzig B, Guesmi F, Sillanpaa M, Hamrouni B (2021) Modelling and optimization of hexavalent chromium removal from aqueous solution by adsorption on low-cost agricultural waste biomass using response surface methodological approach. Water Sci Technol 84:552–575. https:// doi. org/ 10. 2166/ wst. 2021. 233

36. Nambiar AP, Sanyal M, Shrivastav PS (2017) Performance Evaluation and Thermodynamic Studies for the Simultaneous Cloud Point Extraction of Erythrosine and Tartrazine Using Mixed Micelles in Food Samples. Food Anal Methods 10:3471–3480. https:// doi. org/ 10. 1007/ s12161- 017- 0923-1

37. Guedidi H, Lakehal I, Reinert L et al (2020) Removal of ionic liquids and ibuprofen by adsorption on a microporous activated carbon: Kinetics, isotherms, and pore sites. Arab J Chem 13:258–270. https:// doi. org/ 10. 1016/j. arabjc. 2017. 04. 006

38. Januszewicz K, Kazimierski P, Klein M et al (2020) Activated Carbon Produced by Pyrolysis of Waste Wood and Straw for Potential Wastewater Adsorption. Materials 13:2047. https:// doi.org/ 10. 3390/ ma130 92047

39. Ceylan S, Topcu Y (2014) Pyrolysis kinetics of hazelnut husk using thermogravimetric analysis. Bioresour Technol 156:182–188. https:// doi. org/ 10. 1016/j. biort ech. 2014. 01. 040

40. Martin-Lara MA, Blazquez G, Ronda A, Calero M (2016) Kinetic study of the pyrolysis of pine cone shell through non-isothermal thermogravimetry: Effect of heavy metals incorporated by biosorption. Renew Energy 96:613–624. https:// doi. org/ 10. 1016/j.renene. 2016. 05. 026

41. Ozcimen D, Ersoy-Mericboyu A (2010) Adsorption of Copper(II) Ions onto Hazelnut Shell and Apricot Stone Activated Carbons. Adsorpt Sci Technol 28:327–340. https:// doi. org/ 10. 1260/ 0263-6174. 28.4. 327

42. Chen X, Tao J, Sun P et al (2022) Effect of calcination on the adsorption of Chifeng zeolite on Pb2+ and Cu2+. Int J Low-Carbon Technol 17:462–468. https://d oi. org/ 10. 1093/ ijlct/ ctac0 06

43. Wang L, Alsaker N, Skreiberg O, Hovd B (2017) Effect of carbonization conditions on CO2 gasification reactivity of biocarbon. Energy Procedia 142:932–937. https:// doi. org/ 10. 1016/j. egypro.2017. 12. 149

44. Hopkins D, Hawboldt K (2020) Biochar for the removal of metals from solution: A review of lignocellulosic and novel marine feedstocks. J Environ Chem Eng 8:103975. https:// doi. org/ 10. 1016/j.jece. 2020. 103975

45. Shrestha D, Rajbhandari A (2021) The effects of different activating agents on the physical and electrochemical properties of activated carbon electrodes fabricated from wood-dust of Shorea robusta. Heliyon 7:e07917. https:// doi. org/ 10. 1016/j. heliy on.2021. e07917

46. Canales-Flores RA, Prieto-Garcia F (2020) Taguchi optimization for production of activated carbon from phosphoric acid impregnated agricultural waste by microwave heating for the removal of methylene blue. Diam Relat Mater 109:108027. https:// doi. org/10. 1016/j. diamo nd. 2020. 108027

47. Ahsan MdA, Islam MdT, Hernandez C et al (2018) Biomass conversion of saw dust to a functionalized carbonaceous materials for the removal of Tetracycline, Sulfamethoxazole

and Bisphenol A from water. J Environ Chem Eng 6:4329-4338. https:// doi. org/10. 1016/j. jece. 2018. 06. 040

48. Wang S, Zhu Z (2007) Effects of acidic treatment of activated carbons on dye adsorption. Dyes Pigments 75:306-314. https://doi. org/ 10. 1016/j. dyepig. 2006. 06. 005

49. Banerjee S, Chattopadhyaya MC (2017) Adsorption characteristics for the removal of a toxic dye, tartrazine from aqueous solutions by a low cost agricultural by-product. Arab J Chem 10:S1629-S1638. https:// doi. org/ 10. 1016/j. arabjc. 2013. 06. 005

50. Lewoyehu M (2021) Comprehensive review on synthesis and application of activated carbon from agricultural residues for the remediation of venomous pollutants in wastewater. J Anal Appl Pyrolysis 159:105279. https:// doi. org/ 10. 1016/j. jaap. 2021. 105279

51. Jawad AH, Abd Rashid R, Ismail K, Sabar S (2017) High surface area mesoporous activated carbon developed from coconut leaf by chemical activation with H 3 PO 4 for adsorption of methylene blue. Desalination Water Treat. https:// doi. org/ 10. 5004/ dwt. 2017.20571

52. Ramage MH, Burridge H, Busse-Wicher M et al (2017) The wood from the trees: The use of timber in construction. Renew Sustain Energy Rev 68:333-359. https:// doi. org/ 10. 1016/j. rser. 2016. 09. 107

53. El Hajam M, Kandri NI, Harrach A, Zerouale A (2019) Physicochemical characterization of softwood waste “Cedar” and hardwood waste “Mahogany”: comparative study. Mater Today Proc 13:803-811

54. Jaouadi M (2021) Characterization of activated carbon, wood sawdust and their application for boron adsorption from water. Int Wood Prod J 12:22-33. https:// doi. org/ 10. 1080/ 20426 445. 2020.17856 05

55. Sieliechi JM, Thue PS (2015) Removal of paraquat from drinking water by activated carbon prepared from waste wood. Desalination Water Treat 55:986-998. https:// doi. org/ 10. 1080/ 19443 994. 2014.922504

56. Fan L, Zhang Y, Li X et al (2012) Removal of alizarin red from water environment using magnetic chitosan with Alizarin Red as imprinted molecules. Colloids Surf B Biointerfaces 91:250-257. https:// doi. org/ 10. 1016/j. colsu rfb. 2011. 11. 014

57. Management J of ES and, Akpomie K, Onoabedje E et al (2017) Attenuation of Methylene Blue From Aqua-media on Acid Activated Montmorillonite of Nigerian Origin. J Environ Sci Manag 20. https:// doi. org/ 10. 47125/ jesam/ 2017_2/ 03

58. Gautam RK, Gautam PK, Banerjee S et al (2015) Removal of tartrazine by activated carbon biosorbents of Lantana camara: Kinetics, equilibrium modeling and spectroscopic analysis. J Environ Chem Eng 3:79–88. https:// doi. org/ 10. 1016/j. jece. 2014. 11. 026

59. Rashid I, Salman S, Kareem Mohammed P, Mahdi Y (2022) Green Synthesis of Nickle Oxide Nanoparticles for Adsorption of Dyes. Sains Malays 51:533–546. https:// doi. org/ 10. 17576/jsm- 2022- 5102- 17

60. Musthapa SMBH, Shams S, Reddy Prasad DM (2023) Removal of pollutants from wastewater using activated carbon from durian peel. IOP Conf Ser Earth Environ Sci 1135:012001. https:// doi.org/ 10. 1088/ 1755- 1315/ 1135/1/ 012001

61. Fat’ hi AM, Ali AH (2022) Effect of adsorption conditions on the removal of lead (II) using sewage sludge as adsorbent material. J Eng Sustain Dev 26:1–9. https:// doi. org/ 10. 31272/ jeasd. 26.3.1

62. Rzig B, Guesmi F, Sillanpaa M, Hamrouni B (2022) Biosorption potential of olive leaves as a novel low-cost adsorbent for the removal of hexavalent chromium from wastewater. Biomass Convers Biorefinery. https:// doi. org/ 10. 1007/ s13399- 022- 03356-6

63. Touihri M, Guesmi F, Hannachi C et al (2021) Single and simultaneous adsorption of Cr(VI) and Cu (II) on a novel Fe3O4/pine cones gel beads nanocomposite: Experiments, characterization and isotherms modeling. Chem Eng J 416:129101. https:// doi.org/ 10. 1016/j. cej. 2021. 129101

64. Huynh P-T, Nguyen N-T, Van HN et al (2020) Modeling and optimization of biosorption of lead (II) ions from aqueous solution onto pine leaves (Pinus kesiya) using response surface methodology. Desalination Water Treat 173:383–393. https:// doi. org/ 10.5004/ dwt. 2020. 24807

65. Lawal IA, Klink M, Ndungu P (2019) Deep eutectic solvent as an efficient modifier of low-cost adsorbent for the removal of pharmaceuticals and dye. Environ Res 179:108837. https:// doi. org/ 10.1016/j. envres. 2019. 108837

66. Sahnoun S, Boutahala M (2018) Adsorption removal of tartrazine by chitosan/polyaniline composite: Kinetics and equilibrium studies. Int J Biol Macromol 114:1345–1353. https:// doi. org/ 10.1016/j. ijbio mac. 2018. 02. 146

67. Ben Khalifa E, Rzig B, Chakroun R et al (2019) Application of response surface methodology for chromium removal by adsorption on low-cost biosorbent. Chemom Intell Lab Syst 189:18–26. https:// doi. org/ 10. 1016/j. chemo lab. 2019. 03. 014

68. Melliti A, Srivastava V, Kheriji J et al (2021) Date Palm Fiber as a novel precursor for porous activated carbon: Optimization, characterization and its application as Tylosin antibiotic scavenger from aqueous solution. Surf Interfaces 24:101047. https:// doi. org/10. 1016/j. surfin. 2021. 101047

69. Dim PE, Mustapha LS, Termtanun M, Okafor JO (2021) Adsorption of chromium (VI) and iron (III) ions onto acid-modified kaolinite: Isotherm, kinetics and thermodynamics studies. Arab J Chem 14:103064. https:// doi. org/ 10. 1016/j. arabjc. 2021. 103064

70. Ramirez Arenas L, Gentile S, Zimmermann S, Stoll S (2021) Nanoplastics adsorption and removal efficiency by granular activated carbon used in drinking water treatment process. Sci Total Environ 791. https:// doi. org/ 10. 1016/j. scito tenv. 2021. 148175

71. Torres-Perez J, Huang Y, Hadi P et al (2018) Equilibrium, Kinetic and Optimization Studies for the Adsorption of Tartrazine in Water onto Activated Carbon from Pecan Nut Shells. Water Air Soil Pollut 229:73. https:// doi. org/ 10. 1007/ s11270- 017- 3680-2

72. Misran E, Bani O, Situmeang EM, Purba AS (2022) Banana stem based activated carbon as a low-cost adsorbent for methylene blue removal: Isotherm, kinetics, and reusability. Alex Eng J 61:1946–1955. https:// doi. org/ 10. 1016/j. aej. 2021. 07. 022

73. Sghaier W, Torkia YB, Bouzid M, Lamine AB (2022) Thermodynamic analysis of cooling cycles based on statistical physics modeling of ethanol adsorption isotherms. Int J Refrig. https://doi. org/ 10. 1016/j. ijref rig. 2022. 05. 022

74. Dawodu MO, Akpomie KG (2016) Evaluating the potential of a Nigerian soil as an adsorbent for tartrazine dye: Isotherm, kinetic and thermodynamic studies. Alex Eng J 55:3211–3218. https://doi. org/ 10. 1016/j. aej. 2016. 08. 008

75. Monser L, Adhoum N (2009) Tartrazine modified activated carbon for the removal of Pb(II), Cd(II) and Cr(III). J Hazard Mater 161:263–269. https:// doi. org/ 10. 1016/j. jhazm at. 2008. 03. 120

76. Khader E, Mohamed TJ, Albayati T (2021) Comparative performance between rice husk and granular activated carbon for the removal of azo tartrazine dye from aqueous solution. Desalination Water Treat 229:372–383. https:// doi. org/ 10. 5004/ dwt. 2021.27374

77. Gautam RK, Jaiswal N, Singh AK, Tiwari I (2021) Ultrasoundenhanced remediation of toxic dyes from wastewater by activated carbon-doped magnetic nanocomposites: analysis of real wastewater samples and surfactant effect. Environ Sci Pollut Res 28:36680–36694. https:// doi. org/ 10. 1007/ s11356- 021- 13256-3

78. Brice DNC, Manga NH, Arnold BS et al (2021) Adsorption of Tartrazine onto Activated Carbon Based Cola Nuts Shells: Equilibrium, Kinetics, and Thermodynamics Studies. Open J Inorg Chem 11:1. https:// doi. org/ 10. 4236/ ojic. 2021. 111001

79. Fatma N, Morched H, Ines B et al (2022) Isolation, characterization and methylene blue adsorption: Application of cellulose from olive sawdust. Korean J Chem Eng 39:760–774. https:// doi. org/10. 1007/ s11814- 021- 0931-0

80. Tony MA (2022) Aquananotechnology: oriented-sawdust waste valorization into magnetic nanocellulosic particles for Synozol Red K-HL sorption prospect. Appl Water Sci 12:199. https:// doi.org/ 10. 1007/ s13201- 022- 01725-0

81. Bartczak P, Wawrzkiewicz M, Borysiak S, Jesionowski T (2022) Cladium mariscus Saw-Sedge versus Sawdust–Efficient Biosorbents for Removal of Hazardous Textile Dye C.I. Basic Blue 3 from Aqueous Solutions. Processes 10:586. https:// doi. org/ 10.3390/ pr100 30586

82. Saifullahi Shehu I, Atika Ibrahim M, Halimah Funmilayo B, Zakariyya Uba Z (2020) Removal of orange G dye from aqueous solution by adsorption: a short review. J Environ Treat Tech 9:318–327. https:// doi. org/ 10. 47277/ JETT/ 9(1) 327

83. Grassi P, Drumm FC, Georgin J et al (2021) Application of Cordia trichotoma sawdust as an effective biosorbent for removal of crystal violet from aqueous solution in batch system and fixed-bed column. Environ Sci Pollut Res 28:6771–6783. https:// doi. org/ 10.1007/ s11356- 020- 11005-6

84. Khasri A, Jamir MRM, Ahmad AA, Ahmad MA (2021) Adsorption of Remazol Brilliant Violet 5R dye from aqueous solution onto melunak and rubberwood sawdust based activated carbon: interaction mechanism, isotherm, kinetic and thermodynamic properties. Desalination Water Treat 216:401–411. https:// doi.org/ 10. 5004/ dwt. 2021. 26852

85. Pathania D, Sharma S, Singh P (2017) Removal of methylene blue by adsorption onto activated carbon developed from Ficus carica bast. Arab J Chem 10:S1445–S1451. https:// doi. org/ 10. 1016/j.arabjc. 2013. 04. 021

86. Yu R, Shi Y, Yang D et al (2017) Graphene Oxide/Chitosan Aerogel Microspheres with Honeycomb-Cobweb and Radially Oriented Microchannel Structures for Broad-Spectrum and Rapid Adsorption of Water Contaminants. ACS Appl Mater Interfaces 9:21809–21819. https:// doi. org/ 10. 1021/ acsami. 7b046 55

87. Rehman A, Park S-J (2019) Environmental remediation by microporous carbon: an efficient contender for CO2 and methylene blue adsorption. J CO2 Util 34:656–667

88. de Lima Barizao AC, Silva MF, Andrade M et al (2020) Green synthesis of iron oxide nanoparticles for tartrazine and Bordeaux red dye removal. J Environ Chem Eng 8:103618. https:// doi. org/10. 1016/j. jece. 2019. 103618

89. Nazir G, Rehman A, Hussain S et al (2021) Heteroatoms-doped hierarchical porous carbons: Multifunctional materials for effective methylene blue removal and cryogenic hydrogen storage. Colloids Surf Physicochem Eng Asp 630:127554. https:// doi. org/ 10.1016/j. colsu rfa. 2021. 127554

90. Chowdhury S, Saha P (2010) Sea shell powder as a new adsorbent to remove Basic Green 4 (Malachite Green) from aqueous solutions: Equilibrium, kinetic and thermodynamic studies. Chem Eng J 164:168–177

91. Foroutan R, Peighambardoust SJ, Esvandi Z et al (2021) Evaluation of two cationic dyes removal from aqueous environments using CNT/MgO/CuFe2O4 magnetic composite powder: A comparative study. J Environ Chem Eng 9:104752. https:// doi. org/ 10.1016/j. jece. 2020. 104752